Süleyman Demirel Üniversitesi
Fen Bilimleri Enstitüsü Dergisi
Cilt 27, Sayı 1, 116-124, 2023

Süleyman Demirel University
Journal of Natural and Applied Sciences
Volume 27, Issue 1, 116-124, 2023

DOI: 10.19113/sdufenbed.1164720

The Role of Forwarding Dynamic (FD) Simulation in Developing New Knee Prosthesis

Şakir ALTINSOY*[1], Noor SALEH[1], Sevil ÖZER[1]

[1]İstanbul Yeni Yüzyıl University, Faculty of Engineering and Architecture, Department of Biomedical Engineering, 34010, İstanbul, Türkiye

(Alınış / Received: 26.08.2022, Kabul / Accepted: 03.01.2023, Online Yayınlanma / Published Online: 25.04.2023)

Keywords
Control moment gyroscope, Gait simulation, Optimization, Neuromuscular model, Trans-femoral amputee, Knee prosthesis

Abstract: Amputees face several gait deficits due to their mechanically passive prostheses' lack of control and power. Of crucial importance among these deficits are those related to balance, as falls and a fear of falling can cause an avoidance of activity that leads to further debilitation. A transfemoral an artificial limb replaces a missing leg above the knee. A transfemoral prosthesis consists of a socket, knee, shank, foot, and mechanism for the suspension. The current 3D neuromuscular model of a healthy person in this study is adjusted to depict a transfemoral amputee with a 3R60. The model is simulated by Matlab 2019b Simulink program with a walking speed of 0.9 m/s and 1.2 m/s. The model's performance is assessed by comparing the distinctions between the healthy model and the amputee to the literature results. The amputee gait simulated is in keeping with the literature, particularly at speeds of 1.2 m/s. The oscillations of the model in the coronal plane are 0.9 m/s, indicating that balance is difficult to maintain. A case study was also conducted with a gyroscope control moment in the prosthetic shank on fall prevention. The gyroscope control moment enhances flexing the knee and extending it to prevent a drop. The step was more balanced with the extra control time whirligig at 1.2 m/s.

Yeni Diz Protezleri Geliştirmede Dinamik Yönlendirme (FD) Simülasyonunun Rolü

Anahtar Kelimeler
Kontrol momenti jiroskopu, Yürüyüş simülasyonu, Optimizasyon, Nöromüsküler model, Transfemoral ampüte, Diz protezi

Öz: Ampüte bireyler mekanik olarak pasif protezlerinin kontrol ve güç eksikliğinden dolayı çeşitli yürüme sorunları ile karşı karşıyadırlar. Bu sorunların arasında hayati önem taşıyanlar ise denge ile ilgili olanlardır; zira düşmeler ve düşme korkusu, daha çok güç sarfı gerektiren aktivitelerden kaçınmaya neden olabilmektedir. Transfemoral yapay bir uzuv, diz üstünden eksik olan bir bacağın yerini almaktadır. Bir transfemoral protez, bir yuva, diz, gövde, ayak ve süspansiyon mekanizmasından oluşmaktadır. Bu çalışmada, sağlıklı bir bireyin mevcut 3B nöromüsküler modeli, 3R60'lı bir transfemoral ampüte bireyi betimleyecek şekilde uyarlanmıştır. Bu model, 0,9 m/s ve 1,2 m/s yürüme hızlarında Matlab 2019b Simulink programı ile simüle edilmiştir. Sağlıklı model ile ampüte model arasındaki farklar literatür sonuçlarıyla karşılaştırılarak modelin performansı değerlendirilmiştir. Simüle edilen ampüte yürüyüşü, özellikle 1,2 m/s hızda literatür ile uyumlu bulunmuştur. Modelin koronal düzlemdeki salınımı 0,9 m/s'dir; bu da dengeyi korumanın zor olduğunu göstermektedir. Düşmeyi önleme konusunda protez bacakta bir jiroskop kontrol momenti ile bir örnek çalışma da yapılmıştır. Jiroskop kontrol momenti, düşmeyi önlemek için dizin esnemesini (bükülmesini) ve uzamasını artırmaktadır. 1,2 m/s hızda dönme hareketi (whirligig) için atılan adım, ekstra kontrol süresi sayesinde daha dengeli olmuştur.

1. Introduction

Diabetes mellitus, peripheral vascular diseases, trauma, and explosion-related events increase the risk of amputation of lower extremities [1,2]. The list is top by Diabetes mellitus, with an estimated 552 million amputees by 2030 [3]. Additionally, it has been reported that about 93% of explosion injuries end with amputation [2]. The impact of an amputation exceeds the health aspects to economic, mental, and psychological aspects, especially in the low- and middle-income countries [1,3,4]. In the past three

*Corresponding author: sakir.altinsoy@yeniyuzyil.edu.tr

decades, scientists made great efforts to innovate knee prostheses that may alleviate the suffering of transfemoral (TF) amputees. The well-known microprocessor knee (MPK) such as Ossur Rheo the Otto Bock C-leg, Blatchford's Orion, and Freedom Innovations' Plié were easy to use and succeeded in enhancing the stability and the safety. However, they could not mimic the natural knee perfectly [5].

Literature showed that MPK led to several unwanted outcomes among the transfemoral (TF) amputees, such as high energy consumption compared to healthy people [6–8] and asymmetric gait with the possibility of developing osteoarthritis in the intact limb [9]. TF amputees also experienced falling after trips and slips because of losing control over their knees [10,11]. Therefore, the need for scientific experiments to validate and evaluate the actual performance of all newly developed knee syntheses is inevitable. However, the validation processes are often iterative and expensive in terms of time, effort, and money if applied directly to practical experiences. An initial evaluation of prostheses via forwarding dynamic (FD) simulation is a valuable alternative that may reduce the need to build different prototypes and use participants for intermediate tests. Multiple studies used FD simulation to evaluate a new knee prosthesis [12–16]. Most of these studies compare the results obtained from simulation to the available data of healthy people, which seems logical as one would want the FD simulation's gait to mimic the gait of healthy people. However, there are several shortcomings to the methods that were used. Several studies use an optimal torque generator to drive the model's joints. The primary purpose of this study is to adjust the existing 3D neuromuscular model such that it can be able to represent a TF amputee gait wearing a commonly used prosthesis. The prosthesis is to be selected Otto Bock's 3R60 knee prosthesis model, one of the most sold knee prostheses in the Netherlands). Then, the gait mechanics are simulated to evaluate its resemblance to a real amputee. Forward dynamics simulation can be valuable in the development process. It may lead to a decrease in the need for prototypes and tests. It also offers researchers simulation opportunities to change the prosthesis's design by analyzing various scenarios.

2. Material and Method

2.1. Development of 3D TF amputee model

In this study, we used MATLAB-Simulink [17] and Neuromuscular Library to develop a 3D TF amputee model. A control moment gyroscope (CMG) is embedded in the model for the exploratory research on fall prevention, controlled by using a low- and high-level controller. (Figure 1). The 3D TF amputee model consists of four elements: neurological, muscles, skeleton, and the prosthesis controller. The knee is modelled as three bodies representing the knee's physical components: Top, Body, and Bottom. Geometric locations on each body define the body's relation to each other. Fall prevention consists of three main elements: the CMG, the CMG controller, and the trip detector. The joint torques T_i, calculated from the muscle forces F_j^m, determine how the skeleton moves. Joint angles φ_i and muscle stimulations S_j^m are used to calculate muscle forces. The neurological controller controls the muscle stimulations, calculating the required stimulations based on trunk pitch and angular velocity $\emptyset HAT$, trunk roll angle and angular velocity $\emptyset HAT$, muscle lengths ℓ_j^m, and forces F_j^m. Only the neurological controller gains are optimized during gait optimizations. The distance walked χ_{HAT}, average velocity $Vavg$, the sum of stop torques $\sum T_{st,i}$, metabolic energy E_m, and simulation time t_{sim} are all used in the cost function. A CMG is added to prevent falls. The controller cancels out the shank's angular velocity ω_s during normal walking to minimize the perturbation to the normal gait. Trip detection is based on the magnitude of the anterior-posterior and mediolateral local shank accelerations $\|\ddot{\hat{x}}, \ddot{\hat{y}}\|$. If a trip occurs, a gimbal motor torque τ_{GM} is applied, causing the gimbal motor to rotate and the CMG to have a gyroscopic moment, preventing a fall. The CMG controller τ_{CMG} gains are optimized during fall prevention optimization to minimize the exchanged angular momentum ΔH.

2.1.1. Musculoskeletal model

The Musculoskeletal model was adopted by Song and Geyer's model [18]. The model includes amputating the right thigh and replacing the amputated side with a prosthetic foot and shank. The amputated thigh is shortened to match a TF amputation of 11 cm. The model resembles a human with a length of 1.8 m and a mass of approximately 77 kg, including the prosthetic leg. The joint shave soft joint limits to prevent violating anatomic joint limits. When a joint violates a joint limit, a stop request is exerted on the joint to limit further joint limit violations. Song and Geyer use a soft knee joint limit of 5° [19]. However, during normal gait, this limit is exceeded every gait cycle. So, the model relies on the stopping torque τ_{ST} for further joint limit violation.

2.1.2. Prosthesis model

The prosthetic leg consists of the Otto Bock's 3R60 prosthetic knee, a shank, an ankle, and the foot. The prosthetic shank is a rod with a similar center of mass (COM) location as the intact shank. The prosthetic foot is linked to the prosthetic shank via the prosthetic ankle. This ankle is a simple revolute joint with high stiffness, resembling a rigid ankle. The exact mass and inertia of the prosthetic shank and foot are given in Table 1. The 3R60 knee comprises five axes and two hydraulic elements. The axes and hydraulic elements are linked together so that the joint is polycentric and has two degrees of freedom (DOFs). These two DOFs

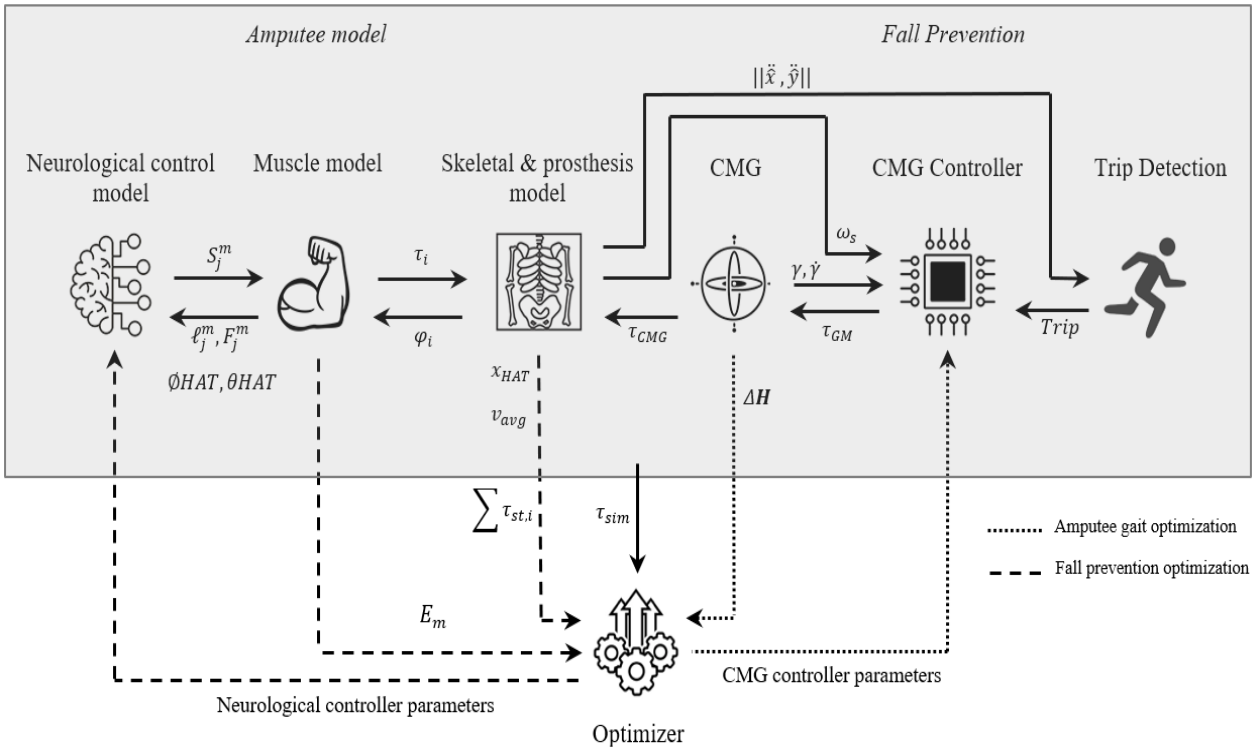

Figure 1. The amputee model is made up by 3 parts: the skeletal and prosthetic model, the muscle model, and the neurological control model. The added control moment gyroscope (CMG) for the fall prevention case study is also depicted in the model

result in different behaviour for stance and swing phases. One hydraulic element is only used during stance phase flexion. The other hydraulic element is mainly used during swing phase flexion. Therefore, the elements have different stiffness and damping characteristics. For the prosthesis model, a multi-body model of the 3R60 knee created by Vandaele [18] is used in Simulink.

2.1.3. Neurological control model

The neurological control model of Song and Geyer [18] is used to control the muscles. The model is supposed to control several gait functions via different reflex modules. Examples of such functionalities are realizing a leg at the landing and preventing knee hyper-extension during stance. A significant circular movement is expected because of the symmetric model of an amputee. The targeted leg angle (TLA) calculator is connected to the integrated lateral positions to overcome this movement. Moreover, the muscles in the amputated side provide insufficient leg clearance information compared to the non-amputated leg. Therefore, the distance between the ankle and hip determines the leg length.

2.2. Control moment gyroscope

For the exploratory research on fall prevention after a trip using a CMG, an obstacle was placed such that the intact leg was tripped in the late swing while walking 1.2 m/s two essential procedures should be carried out:

2.2.1. Detection of trip (intact side)

The accelerometer was placed on the COM of the intact shank for trip detection. The acceleration is sampled at 1000 Hz and then filtered with a high pass and low pass filter with a cut-off frequency of 3 Hz and 80 Hz [22,19]. A simple detection algorithm to classify data comes from acceleration as a trip when the values exceed a certain threshold.

2.2.2. Overcoming of trip (prosthetic side)

Furthermore, a sensor was added to measure the angular velocity of the COM of the prosthetic shank. This sensor is also sampled at 1000 Hz. Finally, the CMG added to the model is embedded in the prosthetic shank. In this step, The CMG is attached below the center of mass of the shank COMs as indicated in [19].

2.2.3. Mechanism of CMG action

According to the size of the CMG, the maximum torque produced by the gimbal motor is set [20]. Therefore, it is needed to reoptimize the muscle-reflex parameters in the amputee gait with an inactive CMG, so it is possible that the model can carry an additional mass. In contrast, two high-level controllers and a feed-forward term have controlled the torque produced by the gimbal motor when the CMG is active. Therefore, the following equation (1) is used to calculate the total gimbal motor torque [21]:

$$\tau_{GM}(t) = I_{ss}\Omega(\omega_{\hat{y}}\, cos(\gamma(t)) - \omega_{\hat{x}}(t)\, sin(\gamma(t))) + \begin{cases} T_w(t), if\ walking \\ T_f(t), if\ trip. \end{cases} \quad (1)$$

2.3. Optimization

In this study, the covariance matrix adaption evolution strategy (CMAES) algorithm was recruited to perform an optimization algorithm [22]. Several parameters were used to optimize the amputee's gait, including the CMG fall prevention controller. In addition, simulation of the model and costing of function was performed. Data for simulation was sampled at 30 Hz. However, data for the fall prevention optimization was sampled at 1000 Hz. The following equation (2) defines the cost function J used for the optimization:

$$J = \underbrace{\alpha.\frac{E_m}{m.\left|\left|\Delta x_{COM}, \Delta y_{COM}\right|\right|}}_{\text{COT}} + \beta.\left|v_{avg} - v_{ref}\right| + \underbrace{\gamma.\sum \tau_s}_{\text{STC}} + \delta.\underbrace{\frac{T_{sim}}{t_{end}} - 1}_{Jt} + \in.\underbrace{||\Delta \boldsymbol{H}(t)||max}_{J_{\Delta H}} \quad (2)$$

CoT: Cost of transport; TVC: Target Velocity Cost; STC: The Stop Torque Cost; Jt: The Time Cost; $J_{\Delta H}$: The Cost of Maximum Exchanged Angular Momentum [22].

Furthermore, different rough terrains were created to test amputee gait optimization. Finally, a self-collision detector was joined to diagnose any collision between the leg chips and stop the simulation when necessary.

2.4. Data processing

For the final gait evaluation, the simulation data obtained from models walking 30s on the flat ground were processed and compared. The acquired data from the model is sampled at 1000 Hz. During post-processing, the data is subdivided into several sections corresponding to a stride. Next, the data underwent linear interpolation, where each section included data points with 0.5 % increments for 0 – 100 %. Then a descriptive analysis was used to present the data as mean and standard deviation (M+SD) per leg. The first four steps are not considered.

2.5. Model validation

In this step, several parameters of the simulated gait of the amputee and healthy model are compared to check whether the model's performance represents a real amputee.

Descriptive analysis was performed, such as the mean, average, and standard deviation of each parameter's absolute symmetry index (ASI).

The mean was calculated by averaging the parameter over all the strides. For the healthy model, the ASI was defined as the difference between the left (L) and right (R) leg gait parameter value of a certain stride: ASI = L − R 0.5(L + R) · 100 %. Consequently, the ASI would be positive values when the left side is larger than the right side.

For the amputee model, the situation is different because the right side is the prosthetic leg, and the left leg is the intact one. Here we compared the parameters of the gait simulation model having active and inactive CMG. The outcome of the comparison may show how much the active CMG can create perturbation to the normal gait.

The healthy model was simulated based on Song and Geyer's [18], with some exceptions, including preoptimizing muscle reflex parameters and changing the muscle expenditure model.

Three parameters, including the joint angles, joint torques, and the ground reaction forces (GRF) used to perform a correlation between the data of simulated healthy gait and data of healthy experimental gait.

3. Results

3.1. Gait simulation

Figure 2(A) and Figure 3(A) present the average joint angles, standard deviation, and the correlation values resulting from the comparison of the data of the healthy human model [23] and the healthy simulated model walking with the same velocity (at 0.9 m/s and 1.2 m/s).

In contrast, Figure 2(B) and Figure 3(B) present the average, standard deviation, and the correlation values of the joint angles obtained from the simulation of the prosthetic leg of the amputee model and the intact leg walking at 0.9 m/s and 1.2 m/s.

The role of active and inactive CMG in controlling the prosthetic leg was shown in Figures 4(A) and 4(B). In addition, the average and standard deviation of the joint angles resulted from the simulation amputee model and intact leg walking on flat ground with 1.2 m/s in both active and inactive CMG (Figure 4-A &B).

3.2. Fall prevention using a control moment gyroscope

The outcome of using the control moment gyroscope (CMG) in fall prevention is illustrated in Figure 5. The data obtained CMG angle, angular velocity, torque, and the exchanged angular momentum are averaged over stride in two situations. Figure 5(A) presents the model's data when it is just moving or walking. At the same time, Figure 5(B) shows the successful fall prevention expressed by the CMG fall prevention controller after exposure to a trip. As shown in figure 5, about 7.1 s where the moment of collision with the obstacle had occurred. However, the time from t = 7.4 s and t = 7.9 s reported the activity of the fall prevention controller.

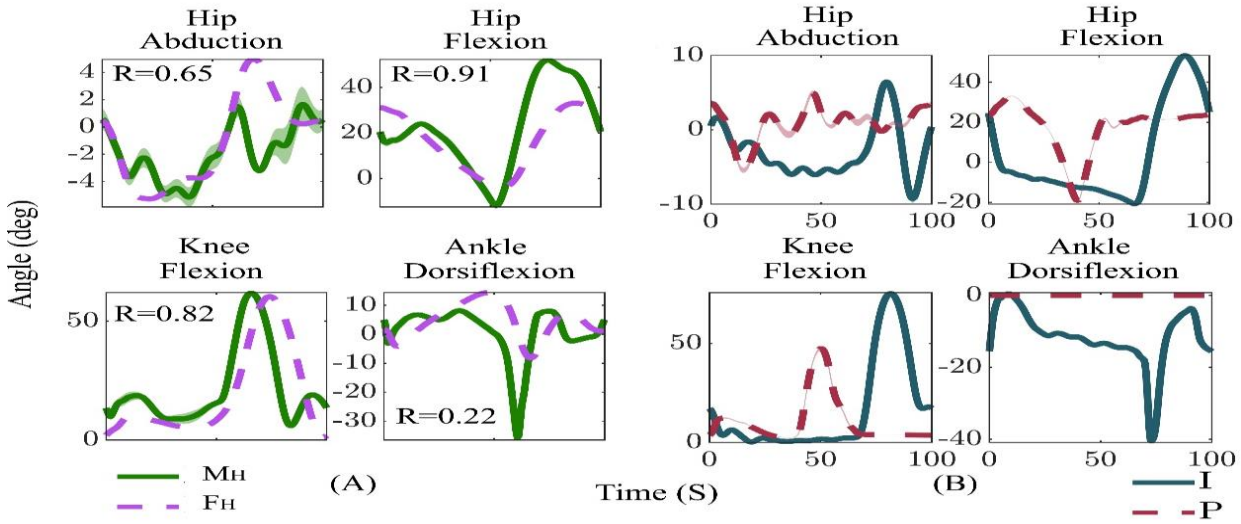

Figure 2. Average joint angles and standard deviation during a stride of (a) a healthy model (M_H) compared to data from Fukuchi (F_H) [23] and (b) for the intact (I) and prosthetic (P) leg of the amputee model walking on flat ground with 0.9 m/s.

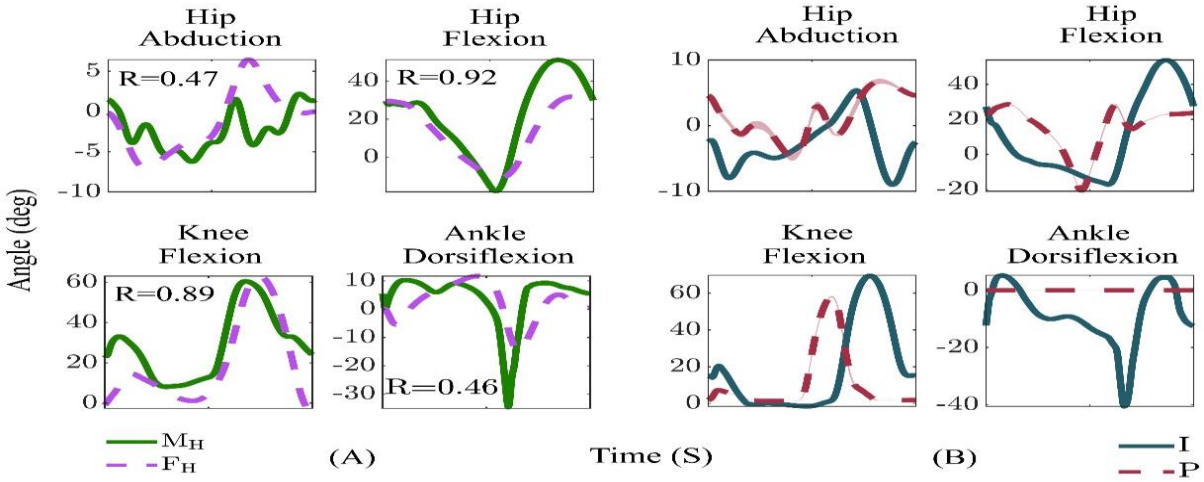

Figure 3. Average joint angles and standard deviation during a stride of (a) a healthy model (M_H) compared to data from Fukuchi (F_H) [23], and (b) for the intact (I) and prosthetic (P) leg with active CMG of the amputee model walking on flat ground with 1.2 m/s

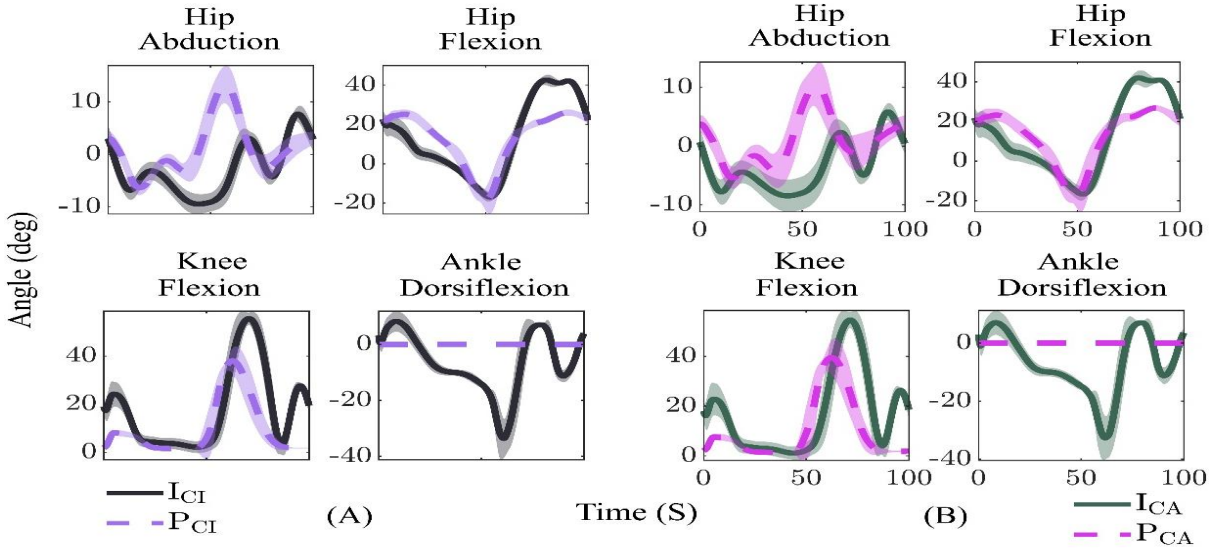

Figure 4. Average joint angles and standard deviation during a stride of (A) for the intact (I_{CI}) and prosthetic (P_{CI}) with inactive CMG, and (B) for the intact (I_{CA}) and prosthetic (P_{CA}) leg with active CMG of the amputee model walking on flat ground with 1.2 m/s.

Table 1. Shows the results of model validation obtained from the simulations of the Healthy model (intact leg) and amputee model (Prosthesis leg). The average and standard deviation parameters include stance time, swing time, double stance time, step time, and step length

		0.9 m/s		1.2 m/s	
		Mean	**ASI**	**Mean**	**ASI**
t_{St} (s)	M_H	0.69 (0.01)	0.23 (1.47)	0.61 (0.00)	-0.12 (0.72)
	I	0.92 (0.01)	48.60 (0.65)	0.67 (0.01)	26.26 (0.65)
	P	0.59 (0.00)		0.49 (0.00)	
	I_{CI}			0.65 (0.08)	7.86 (9.69)
	P_{CI}			0.64 (0.02)	
	I_{CA}			0.68 (0.09)	13.72 (11.31)
	P_{CA}			0.63 (0.02)	
t_{Sw} (s)	M_H	0.48 (0.00)	- 0.03 (1.37)	0.49 (0.00)	0.13 (0.71)
	I	0.35 (0.00)	- 64.28 (1.19)	0.37 (0.00)	-36.61 (0.86)
	P	0.72 (0.01)		0.52 (0.01)	
	I_{CI}			0.47 (0.01)	-12.62 (13.23)
	P_{CI}			0.53 (0.06)	
	I_{CA}			0.43 (0.01)	-15.58 (11.84)
	P_{CA}			0.55 (0.07)	
t_{DS} (s)	M_H	0.09 (0.00)	- 0.31 (1.85)	0.08 (0.00)	0.05 (1.82)
	I	0.08 (0.00)	- 17.56 (1.49)	0.07 (0.00)	26.37 (3.71)
	P	0.09 (0.00)		0.05 (0.00)	
	I_{CI}	P_{CI}		0.10 (0.01)	22.60 (13.13)
	P_{CI}	I_{CA}		0.08 (0.01)	
	I_{CA}	P_{CI}		0.09 (0.02)	31.78 (15.14)
	P_{CA}	I_{CA}		0.06 (0.01)	
t_S (s)	M_H	0.63 (0.01)	- 0.17 (1.11)	0.53 (0.00)	0.16 (0.42)
	I	0.48 (0.00)	- 57.03 (1.29)	0.48 (0.00)	-27.85 (0.89)
	P	0.79 (0.01)		0.59 (0.01)	
	I_{CI}			0.53 (0.01)	-8.35 (10.27)
	P_{CI}			0.59 (0.07)	
	I_{CA}			0.57 (0.02)	-11.46 (11.78)
	P_{CA}			0.58 (0.08)	
ℓ_S(s)	M_H	0.52 (0.01)	0.49 (2.94)	0.65 (0.01)	-0.36 (1.75)
	I	0.44 (0.00)	- 51.28 (1.21)	0.58 (0.01)	-21.94 (1.69)
	P	0.71 (0.00)		0.73 (0.00)	
	I_{CI}			0.67 (0.12)	-7.64 (5.81)
	P_{CI}			0.73 (0.03)	
	I_{CA}			0.66 (0.13)	-2.47 (13.63)
	P_{CA}			0.65 (0.04)	

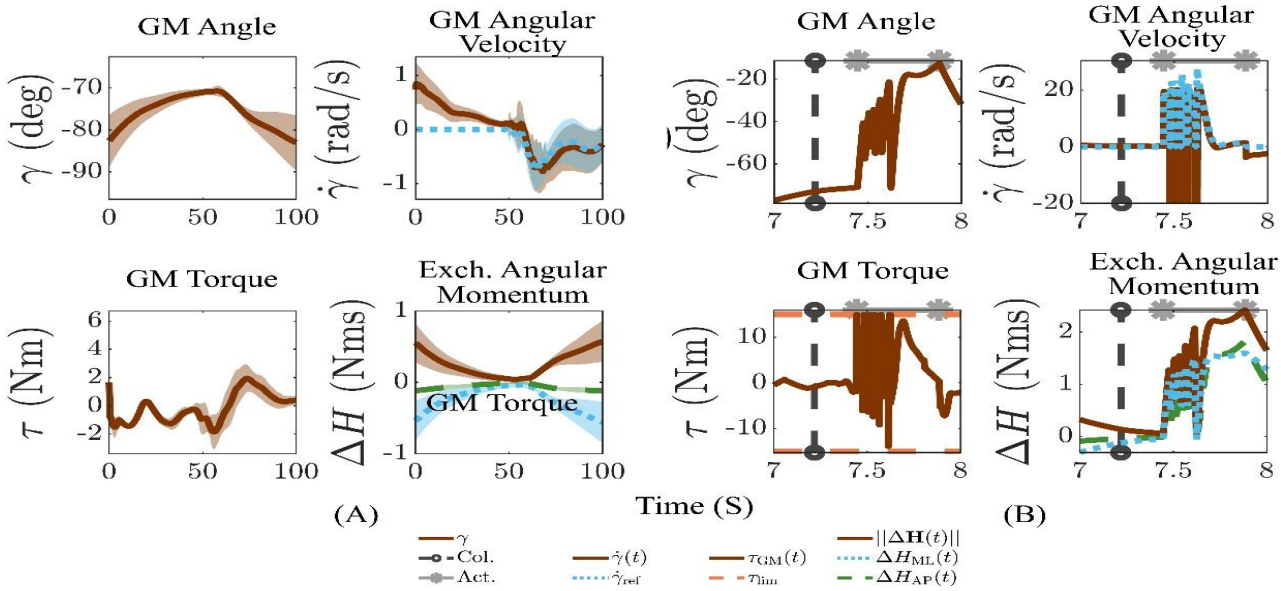

Figure 5. Amputee model walking with CMG at 1.2 m/s with (a) the average data for the control moment gyroscope during a stride, and (b) the control response for successful fall prevention. The moment of collision (Col.) with the obstacle is around t = 7.2 s. The time the fall prevention response is active (Act.) are indicated in the fall prevention plots, which is between t = 7.4 s and t = 7.9 s.

Table 2. Shows the descriptive analysis (the average and standard deviation) of all parameters and the ASI resulting from the simulations of the healthy and amputee models

		0.9 m/s		1.2 m/s	
		Mean	**ASI**	**Mean**	**ASI**
$P_{a,max}$ (W/kg)	M_H	1.21 (0.08)	-1.23 (7.93)	1.02 (0.02)	0.31 (1.44)
	I	2.07 (0.07)	-	2.87 (0.06)	-
	I_{CI}			2.91 (0.51)	-
	I_{CA}			2.65 (0.60)	-
p_{Xb} (Ns/kg)	M_H	-0.31 (0.02)	2.19 (10.39)	-0.33 (0.02)	-1.04 (6.79)
	I	-0.35 (0.01)	13.31 (1.89)	-0.51 (0.01)	101.87 (4.92)
	P	-0.31 (0.01)		-0.19 (0.01)	
	I_{CI}			-0.34 (0.06)	31.79 (21.63)
	P_{CI}			-0.24 (0.05)	
	I_{CA}			-0.31 (0.06)	54.88 (36.24)
	P_{CA}			-0.23 (0.06)	
p_{Xp} (Ns/kg)	M_H	0.23 (0.01)	- 1.89 (7.16)	0.27 (0.01)	0.42 (4.58)
	I	0.69 (0.01)	151.82 (1.06)	0.42 (0.01)	73.14 (3.76)
	P	0.08 (0.00)		0.19 (0.01)	
	I_{CI}			0.45 (0.03)	72.71 (13.14)
	P_{CI}			0.23 (0.02)	
	I_{CA}			0.44 (0.05)	71.74 (11.81)
	P_{CA}			0.17 (0.03)	
p_z (Ns/kg)	M_H	5.92 (0.05)	0.15 (1.04)	5.48 (0.04)	- 0.12 (1.03)
	I	8.14 (0.07)	51.63 (0.84)	6.25 (0.05)	37.39 (0.95)
	P	1.76 (0.03)		4.32 (0.04)	
	I_{CI}			5.89 (0.69)	15.46 (9.32)
	P_{CI}			5.01 (0.10)	
	I_{CA}			6.23 (0.77)	19.37 (12.09)
	P_{CA}			5.02 (0.12)	

4. Discussion and Conclusion

In this study, a 3D neuromuscular model was readjusted to mimic TF amputee wearing the Otto Bock 3R60 knee prosthesis. The simulation outcome showed a similarity between the amputee gait and the gait of a TF amputee when walking at a velocity of 0.9 m/s and 1.2 m/s. However, asymmetric characteristics and contra-lateral vaulting were also reported in TF amputees. Likewise, to the findings of [24], the vaulting characteristic was also seen in the maximum ankle power through a single stance. In our study, we found that the intact ankle of a TF amputee showed greater vaulting characteristics than the ankle in healthy humans. Moreover, the vaulting characteristic appeared in the simulated gait and for both velocities (0.9 m/s and 1.2 m/s).

Similar to findings reported by [25,26], the simulated amputee gait showed similar positive or negative asymmetry at the velocity of 1.2 m/s. The stance time was longer in the intact leg than in the prosthetic leg, while the step length, step time, and the swing time were longer in the prosthetic leg than in the intact leg. Regarding the ASI and the change in ASI between different velocities, the magnitude was more significant than the results reported by [25,26].

In fact, the simulated gait moving at the velocity of 0.9 m/s reported deviations compared to earlier studies. Considering the stance time when the model is stepping from the prosthetic leg onto the intact leg, our findings agreed with Nolan [25], where the stance time has doubled. However, Schaarschmidt [26] found that stance time has doubled if the model steppes from the intact leg to the prosthetic leg.

Furthermore, we found that the average anterior-posterior propelling impulse was smaller in the prosthetic leg than the braking impulse. Such a finding was in line with that mentioned by Nolan [25], but was opposite to findings mentioned by [26].

Different velocities showed various changes in the asymmetry values. In our study, the change in asymmetry for swing time was two times longer than the result reported by [25]. The change in the asymmetry of both stance and step time was much more significant than the result of [25,26].

Another finding was related to the mean impulse asymmetries of the simulation, which were dissimilar across different velocities. However, [25,26] reported that in the simulation, the mean impulse asymmetries were similar across all velocities [25,26].

In this study, except for the joint torque correlation, the values for the joint angle and GRF correlation factor in the simulated healthy gait at 1.2m/s were similar to those produced by [18]. In contrast, except for the hip abduction angle correlation, all other correlation factors were worse in the simulated healthy gait at 0.9 m/s. Similar to findings reported by [18], we also found that the difference in joint torque

correlation is quite similar. The reason behind such findings may be attributed to changes in the soft joint limit, which causes different joint torques. Moreover, the ankle joint was designed as a 1 DOF revolute joint, which justifies the reason behind the low correlation.

The simulated gait of the amputee and healthy model reported different results from the previously published research at the velocity of 0.9 m/s [25,26]. It is most probably related to simplification procedures in the coronal plane. The consequences were difficulties in controlling balance at the lower velocities. Despite the optimization procedures to produce an optimal gait, the designed model lacks the human factor, which may result in some deviation from reality. Similarly, [26] reported that amputees are most likely to be cautious when stepping with the prosthetic leg [26] compared to models with no fear and no cautions.

Although the 3R60 prosthetic knee showed similar characteristics to findings reported by [27], the maximum swing-phase flexion was lower than [27] at 0.9 m/s and 1.2 m/s. The 3R60 prosthetic knee seems sensitive and adequately accurate to simulate the gait of a TF amputee.

Among the problems experienced in the model was the difficulty in the lateral control. This problem arose when we compared the gait simulations on rough terrain and changed the model. The solution to such a problem was to reoptimize the gait parameters.

In conclusion, the features of the 3D neuromuscular simulated gait of the TF amputee model wearing the Otto-bock 3R60 knee prosthesis coincides with previously discussed models, especially when the model is moving at the velocity of 1.2 m/s. However, when the velocity comes down to 0.9 m/s, the model may complain of some deviations in the amputee and the healthy model, which requires further research in modelling muscle structure and nerve control of humans. Furthermore, the embedded control moment gyroscope prevented falls after a trip and improved the gait symmetry at a velocity of 1.2 m/s.

Declaration of Ethical Code

In this study, we undertake that all the rules required to be followed within the scope of the "Higher Education Institutions Scientific Research and Publication Ethics Directive" are complied with, and that none of the actions stated under the heading "Actions Against Scientific Research and Publication Ethics" are not carried out.

References

[1] Barnes, J. A., Eid, M. A., Creager, M. A., Goodney, P. P. 2020. Epidemiology and Risk of Amputation in Patients with Diabetes Mellitus and Peripheral Artery Disease. Arteriosclerosis, Thrombosis, and Vascular Biology, 40(8),1808-1017.

[2] Isaacson, B. M., Weeks, S. R., Pasquina, P. F., Webster, J. B., Beck, J.P., Bloebaum, R. D. 2010. The road to recovery and rehabilitation for injured service members with limb loss: a focus on Iraq and Afghanistan, US Army Medical Department Journal. https://pubmed.ncbi.nlm.nih.gov/21181652/ (Erişim Tarihi: 15.03.2022).

[3] Whiting, D. R., Guariguata, L., Weil, C., Shaw, J. 2011. IDF Diabetes Atlas: Global Estimates of the Prevalence of Diabetes for 2011 and 2030. Diabetes Research and Clinical Practice, 94(3), 311-321.

[4] Sahu, A., Sagar, R., Sarkar, S., Sagar, S. 2016. Psychological Effects of Amputation: A Review of Studies from India. Industrial Psychiatry Journal. 25(1), 4.

[5] Campbell, J. H., Stevens, P. M., Wurdeman, S. R. 2020. OASIS 1: Retrospective Analysis of Four Different Microprocessor Knee Types, Journal of Rehabilitation and Assistive Technologies Engineering. 7, 1-10.

[6] Waters, R. L., Perry, J., Antonelli, D.A., Hislop, H. 1976. Energy Cost of Walking of Amputees: The İnfluence of Level of Amputation. J Bone Joint Surg Am, 58(1), 42-46.

[7] Boonstra, A. M., Schrama, J., Fidler, V., Eisma, W. H. 1994. The Gait of Unilateral Transfemoral Amputees. Scandinavian Journal of Rehabilitation Medicine, 26(4), 217-223.

[8] Chin, T., Sawamura, S., Shiba, R., Oyabu, H., Nagakura, Y., Takase, I., Machida, K., Nakagawa, A. 2003. Effect of an Intelligent Prosthesis (IP) on the Walking Ability of Young Transfemoral Amputees: Comparison of IP Users with Able-Bodied People. American Journal of Physical Medicine & Rehabilitation, 82(6), 447-451.

[9] Gailey, R., Allen, K., Castles, J., Kucharik, J., Roeder, M. 2008. Review of Secondary Physical Conditions Associated with Lower-Limb Amputation and Long-Term Prosthesis Use. Journal of Rehabilitation Research and Development, 45(1), 15-30.

[10] Emani, S., Ramasamy, M., Shaari, K. Z. 2019. Discrete Phase-CFD Simulations of Asphaltenes Particles Deposition from Crude Oil in Shell and Tube Heat Exchangers, Applied Thermal Engineering, 149, 105-118.

[11] Crenshaw, J. R., Kaufman, K. R., Grabiner, M. D. 2013. Trip Recoveries of People with Unilateral, Transfemoral or Knee Disarticulation Amputations: Initial Findings, Gait and Posture, 38(3), 534-546.

[12] Shandiz, M. A., Farahmand, F. A., Zohour, H. A. 2010. Dynamic Simulation of the Biped Normal and Amputee Human Gait. In Mobile Robotics: Solutions and Challenges, 2010, 1113-1120.

[13] Van den Bogert, A. J., Samorezov, S., Davis, B.L., Smith, W. A. 2012. Modeling and Optimal Control of an Energy-Storing Prosthetic Knee, Journal of Biomechanical Engineering, 134(5), 1 -8,

[14] Geng, Y., Yang, P., Xu, X., Chen, L. 2012. Design and Simulation of Active Transfemoral Prosthesis. In2012 24th Chinese Control and Decision Conference (CCDC) 2012 May 23, 3724-3728.

[15] Thatte, N., Geyer, H., 2015. Toward Balance Recovery with Leg Prostheses Using Neuromuscular Model Control. IEEE Transactions on Biomedical Engineering, 63(5), 904-913.

[16] Fletcher, M., 2017. Design and validation of a transfemoral amputee walking model with passive prosthesis swing phase control, PhD Thesis. University of Toronto (Canada).

[17] Matlab., 2019. 9.7.0.1190202 (R2019b). Natick, Massachusetts: The MathWorks Inc.

[18] Song, S., Geyer, H., 2015. A neural Circuitry That Emphasizes Spinal Feedback Generates Diverse Behaviours of Human Locomotion. The Journal of Physiology, 593(16), 3493-3511.

[19] Lawson, B. E., Varol, H. A., Sup, F., Goldfarb, M., 2010. Stumble Detection and Classification for an İntelligent Transfemoral Prosthesis. In2010 Annual International Conference of the IEEE Engineering in Medicine and Biology 2010 Aug 31, 511-514.

[20] Jabeen, S., Berry, A., Geijtenbeek, T., Harlaar, J., Vallery, H. 2019. Assisting Gait with Free Moments or Joint Moments on the Swing Leg. In2019 IEEE 16th International Conference on Rehabilitation Robotics (ICORR) 2019 Jun 24, 1079-1084.

[21] Yin, K., Loken, K., Van de Panne, M. 2007. Simbicon: Simple Biped Locomotion Control. ACM Transactions on Graphics (TOG), 26(3), 105-es.

[22] Hansen, N. 2006. The CMA Evolution Strategy: a Comparing Review. Towards a New Evolutionary Computation, 75-102.

[23] Fukuchi, C. A., Fukuchi, R. K., Duarte, M. 2018. A Public Dataset of Overground and Treadmill Walking Kinematics and Kinetics in Healthy İndividuals. Peer, 6, e4640.

[24] Drevelle, X., Villa, C., Bonnet, X., Loiret, I., Fodé, P., Pillet, H. 2014. Vaulting Quantification During Level Walking of Transfemoral Amputees, Clinical Biomechanics, 29(6), 679-83.

[25] Nolan, L., Wit, A., Dudziñski, K., Lees, A., Lake, M., Wychowañski, M. 2003. Adjustments in Gait Symmetry with Walking Speed in Trans-Femoral and Trans-Tibial Amputees, Gait and Posture, 17(2), 142-151.

[26] Schaarschmidt, M., Lipfert, S. W., Meier-Gratz, C., Scholle, H. C., Seyfarth, A. 2012. Functional Gait Asymmetry of Unilateral Transfemoral Amputees, Human Movement Science, 31(4), 907-917.

[27] Blumentritt, S., Scherer, H. W., Wellershaus, U., Michael, J. W. 1997. Design Principles, Biomechanical Data and Clinical Experience with a Polycentric Knee Offering Controlled Stance Phase Knee Flexion: A Preliminary Report, JPO: Journal of Prosthetics and Orthotics, 9(1), 18-24.